This article is published as part of the *Dalton Transactions* themed issue entitled:

Self-Assembly in Inorganic Chemistry

Guest Editors Paul Kruger and Thorri Gunnlaugsson

Published in issue 45, 2011 of *Dalton Transactions*

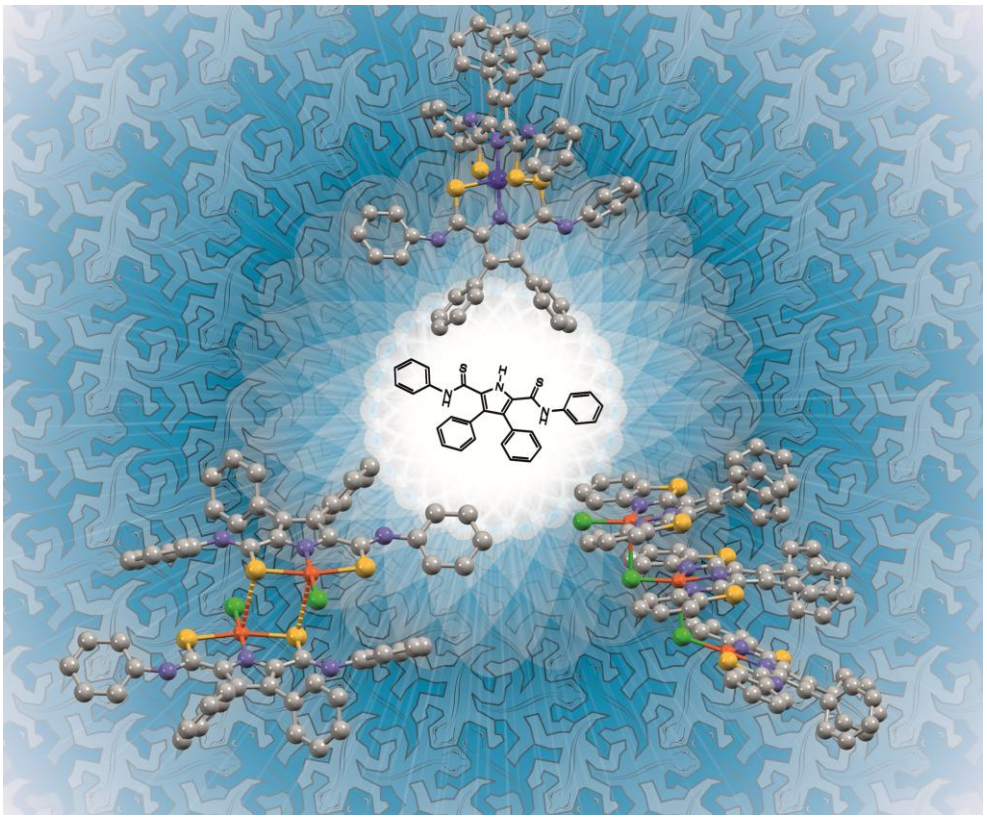

Image reproduced with permission of Mark Ogden

Articles in the issue include:

PERSPECTIVE:

ARTICLES:

Visit the *Dalton Transactions* website for more cutting-edge inorganic and organometallic research
www.rsc.org/dalton

Dalton Transactions

Dynamic Article Links

Cite this: *Dalton Trans.*, 2011, **40**, 12180

www.rsc.org/dalton

PAPER

Clipping and stoppering anion templated synthesis of a [2]rotaxane host system†

Yitong Li,[a] Kathleen M. Mullen,[a,c] João Sardinha,[b] Vítor Félix[b] and Paul D. Beer*[a]

Received 11th May 2011, Accepted 7th July 2011
DOI: 10.1039/c1dt10887e

A new [2]rotaxane host system containing nitro-isophthalamide macrocycle and polyether functionalised pyridinium axle components is prepared *via* clipping and stoppering synthetic methodologies using chloride anion templation. After removing the chloride anion template, ^{1}H NMR titration experiments reveal the unique interlocked host cavity to be highly selective for binding chloride and bromide in preference to basic oxoanions in competitive aqueous solvent mixtures. The rotaxane host system proved to be a superior anion complexant in comparison to the individual macrocycle and axle components. The anion binding affinity of the novel rotaxane is also investigated *via* molecular dynamics simulations and in general the structural data obtained corroborates the experimental solution anion recognition behaviour.

Introduction

Inspired by potential nanotechnological applications as components of molecular machines and switches, the innovative design and construction of interlocked molecules is an area of ever increasing research activity.[1] In spite of this huge interest the potential exploitation of these molecules to function as molecular recognition and sensory reagents has been largely overlooked which is surprising given that their unique, topologically constrained three-dimensional host cavities can be engineered to bind specific guest species during their template-driven syntheses.[2]

With this in mind we have undertaken a research programme with the objective of exploiting the cavities of rotaxanes and catenanes for anion recognition purposes.[3,4] An anion templating strategy has been developed in which a pyridinium chloride ion-pair is used as an axle threading component through an isophthalamide macrocycle for interweaved molecular assembly.[5,6] Herein a new rotaxane host system which contains a nitro-isophthalamide macrocycle and polyether appended pyridinium axle components is described, prepared *via* clipping and stoppering anion templation synthetic methodologies. Anion binding studies reveal the unique interlocked host cavity to be highly selective for binding chloride and bromide in preference to basic oxoanions in competitive aqueous solvent mixtures. Furthermore, computational molecular dynamics simulations corroborate the rotaxane's experimentally observed anion binding preferences.

[a]*Inorganic Chemistry Laboratory, Department of Chemistry, University of Oxford, South Parks Road, Oxford, UK, OX1 3QR. E-mail: paul.beer@chem.ox.ac.uk; Fax: (+44) 1865-272-690*
[b]*Departamento de Química, CICECO and Secção Autónoma de Ciências da Saúde Universidade de Aveiro, 3810-193, Aveiro, Portugal. E-mail: vitor.felix@ua.pt; Fax: (+351) 234 370084*
[c]*Current address: Chemistry, Faculty of Science and Technology, Queensland University of Technology, G. P. O. Box 2434, Brisbane, 4001, Australia. E-mail: kathleen.mullen@qut.edu.au; Fax: +61-7-3864-1804*

† Electronic supplementary information (ESI) available: Experimental procedures, characterisation and selected titration data. See DOI: 10.1039/c1dt10887e

Results and discussion

Synthetic strategy

Two complementary synthetic strategies were employed for the anion templated synthesis of a new [2]rotaxane, clipping (Scheme 1a) and stoppering (Scheme 1b).

The macrocycle, macrocycle precursor, axle and threading components required for the respective synthetic procedures are shown in Scheme 1. It was anticipated that either ring closing metathesis of a vinyl appended isophthalamide receptor encircling a stoppered pyridinium chloride axle, or urethane stoppering of a pyridinium chloride thread-isophthalamide macrocycle pseudorotaxane assembly, would generate the target [2]rotaxane.

Bis-vinyl macrocycle precursor **1** and macrocycle **2** were prepared using modified literature procedures.[5] The synthetic route used to prepare the new threading component **3**-Cl is shown in Scheme 2. Diethylene glycol was stirred with 0.25 equivalents of tosyl chloride to give the mono-tosylated derivative **5** in 74% yield after column chromatography. Compound **5** was then refluxed with 4-hydroxyphenylacetamide in the presence of potassium carbonate to give the polyether derivative **6** in good yield. Hydrolysis of the secondary amide group was achieved with sodium hydroxide in an EtOH/H_2O solvent mixture to give amine **7** which was then reacted with 3,5-pyridinedicarboxylic acid using *N*-(3-dimethylaminopropyl)-*N*′-ethylcarbodiimide hydrochloride (EDC·HCl) and 1-hydroxybenzotrizaole (HOBt) as coupling reagents to give the bis-amide compound **8** in 47%

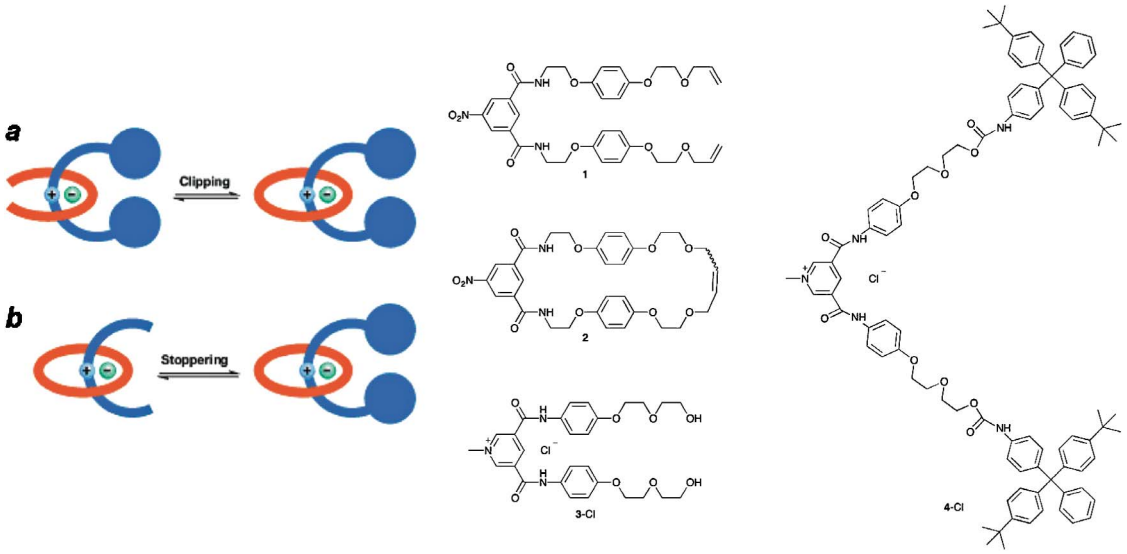

Scheme 1 (a) Clipping and (b) stoppering strategies of anion templated isophthalamide-pyridinium rotaxane synthesis.

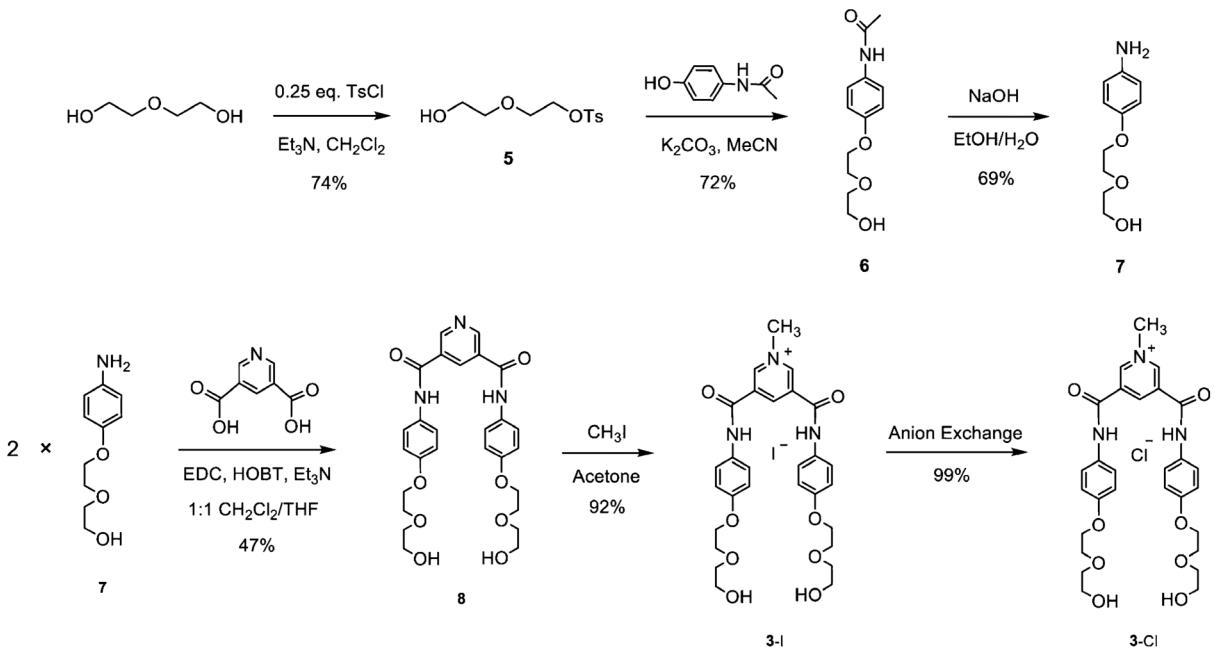

Scheme 2 Synthesis of pyridinium chloride ion-pair thread **3**-Cl.

yield. Alkylation of the pyridine ring with iodomethane gave the pyridinium iodide derivative **3**-I in 92% yield. The pyridinium chloride thread **3**-Cl could be obtained in quantitative yield using an Amberlite chloride exchange column.

The synthetic route used to synthesise the stoppered pyridinium thread needed for rotaxane synthesis using a clipping methodology is shown in Scheme 3. Two equivalents of isocyanate terphenyl stopper compound **9**[7] were stirred with **8** and a catalytic amount of dibutyltin dilaurate in dichloromethane to afford **10** in 73% yield. This was then alkylated using trimethyloxonium tetrafluoroborate to afford the pyridinium tetrafluoroborate derivative **4**-BF_4 in 92% yield. Anion exchange was achieved by washing **4**-BF_4 with a saturated aqueous solution of NH_4Cl to give stoppered pyridinium chloride axle **4**-Cl in quantitative yield.

Rotaxane synthesis *via* the clipping method

Initial rotaxane synthesis attempts focused on a clipping strategy, in which ring closing metathesis of a vinyl appended macrocycle precursor around the stoppered pyridinium thread **4**-Cl would afford the desired interlocked architecture. Equimolar amounts of bis-vinyl appended macrocycle precursor **1** and stoppered pyridinium chloride axle **4**-Cl were mixed in dry CH_2Cl_2. Grubbs' 2nd generation catalyst (5% by weight)[8] was added to the mixture and the rotaxane chloride salt **11**-Cl was isolated in 55% yield by column chromatography using 96 : 4 CH_2Cl_2/MeOH as eluent (Scheme 4).

The ^{1}H NMR spectrum of rotaxane **11**-Cl in $CDCl_3$ as compared with that of macrocycle **2** and axle **4**-Cl is shown

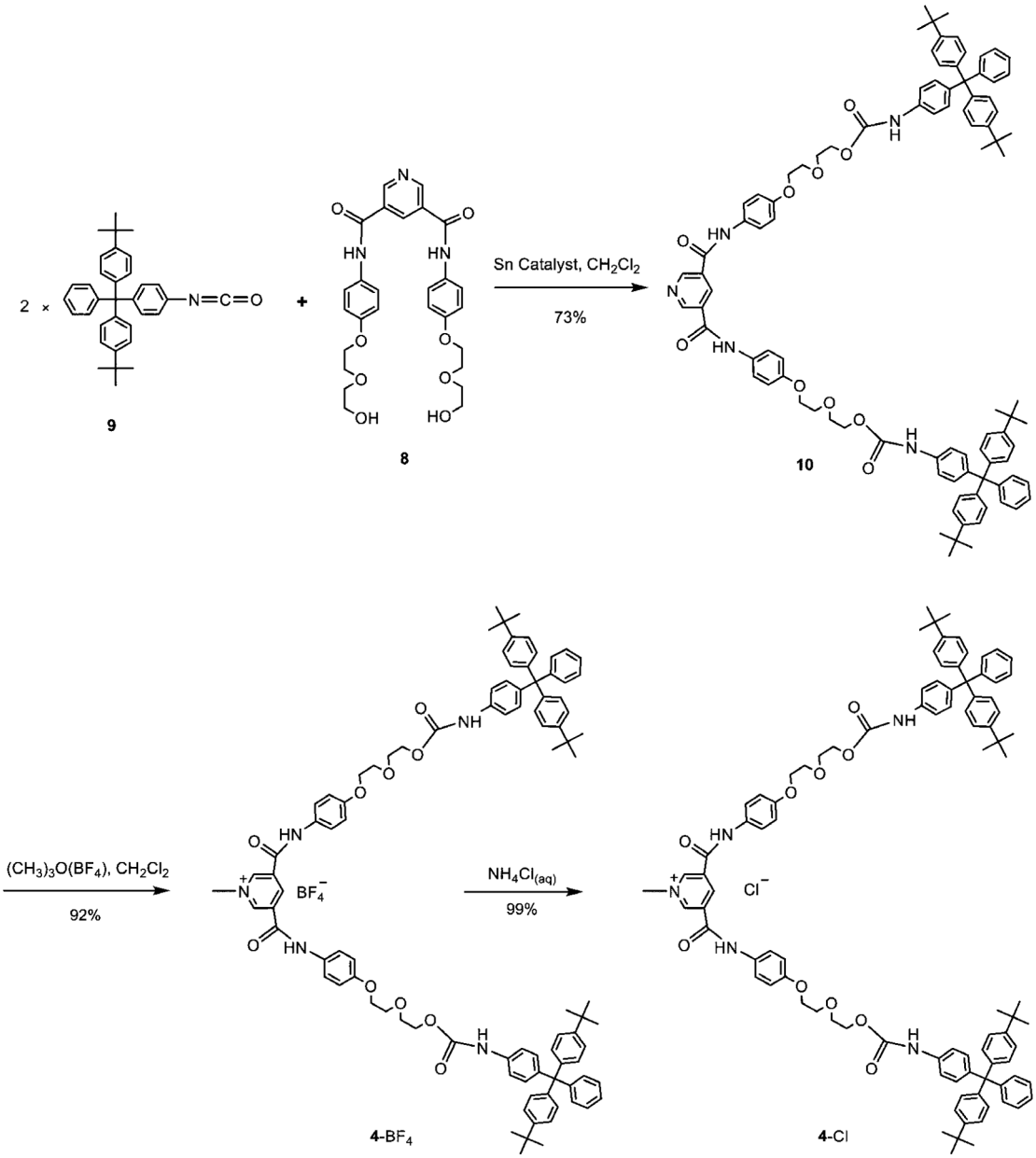

Scheme 3 Synthesis of stoppered pyridinium chloride ion-pair axle **4**-Cl.

in Fig. 1. Significant upfield shifts and splitting of the nitro-isophthalamide macrocyclic hydroquinone protons H_e ($\Delta\delta$ = 0.34 ppm) and H_f ($\Delta\delta$ = 0.63 ppm) was observed in the spectrum of **11**-Cl. This is indicative of π–π stacking between the positively charged pyridinium motif and the hydroquinone aromatic rings, which is characteristic of interpenetration.[9] Downfield shifts were also observed for the macrocyclic nitro-isophthalamide amide H_i ($\Delta\delta$ = 1.54 ppm) and aryl protons H_j ($\Delta\delta$ = 0.68 ppm) and H_k ($\Delta\delta$ = 0.13 ppm) which is indicative of anion binding. Moreover, an upfield shift of the pyridinium amide axle protons H_d ($\Delta\delta$ = 0.94 ppm) was observed. This is a result of the polarisation of the chloride anion towards the amide hydrogen bond donor groups of the macrocycle which in turn reduces the strength of the hydrogen bonding interaction between the anion and the amide groups of the pyridinium cation axle. The disappearance of the characteristic multiplets associated with the vinyl protons of reactant **1** and the appearance of a singlet at 6.09 ppm corresponding to the cyclised double bonds (see ESI†) is typical of a successful RCM reaction. Furthermore, a downfield shift was observed for *N*-methyl pyridinium proton H_a ($\Delta\delta$ = 0.24 ppm) of the rotaxane which is indicative of hydrogen bonding interactions between the methyl group of the pyridinium axle and the macrocyclic polyether ring.

The structure of rotaxane **11**-Cl was further investigated using ROESY ^{1}H–^{1}H NMR spectroscopy in $CDCl_3$. The spectrum shown in Fig. 2 highlights through-space proton–proton correlation signals arising from aromatic stacking interactions between macrocycle and axle components of the rotaxane. Near in space correlations between the *para*-pyridinium H_c and aryl protons H_e and H_f of the pyridinium axle molecule and the hydroquinone

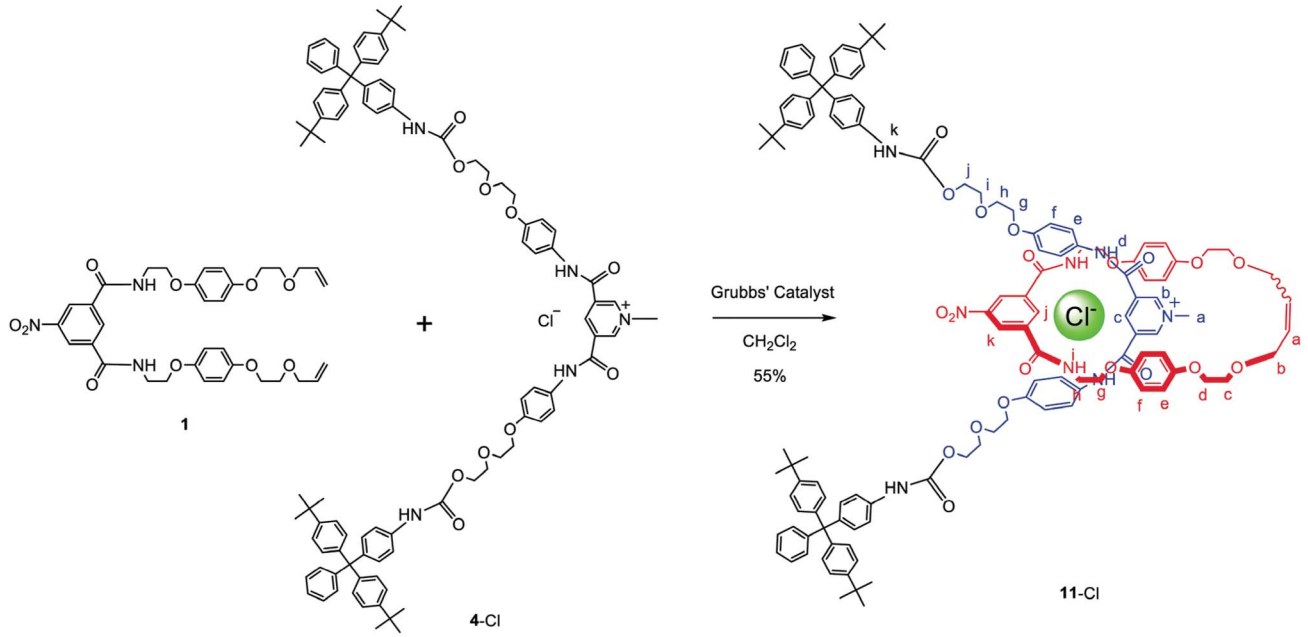

Scheme 4 Synthesis of rotaxane **11**-Cl *via* clipping strategy.

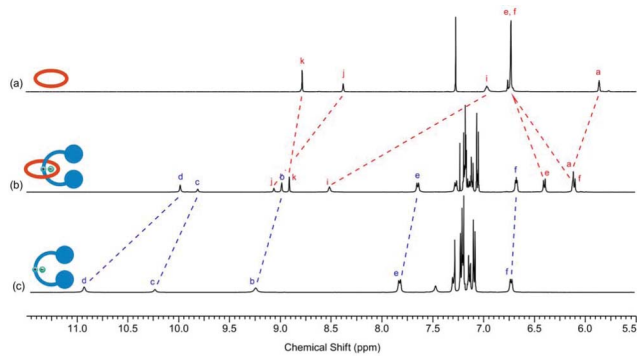

Fig. 1 Selected region of the ^{1}H NMR (500 MHz, 298 K, $CDCl_3$) spectra of (a) macrocycle **2**, (b) rotaxane **11**-Cl and (c) thread molecule **4**-Cl. For proton labelling see Scheme 4.

proton H_e of the macrocycle is a result of stabilising π–π stacking interactions between the positively charged electron-deficient pyridinium motif and the macrocyclic electron-rich hydroquinone groups. Similarly, through-space correlations between the aryl protons (H_e and H_f) of the axle molecule and the macrocyclic nitro-isophthalamide protons (H_j and H_k) are indicative of a π–π stacking interaction between the electron-rich aryl groups and the electron-deficient nitro-isophthalamide group of the macrocycle. In addition, strong through space interactions between pyridinium *N*-methyl protons H_a and polyether protons (H_a, H_b and H_c) were observed indicative of hydrogen bonding interactions between the pyridinium methyl group and the oxygen atoms of the macrocyclic polyether.

Rotaxane synthesis *via* the stoppering method

In order to assess whether the synthesis of the same rotaxane could be achieved *via* a stoppering method, anion templated pseudorotaxane formation between **3**-Cl and **2** was investigated initially by ^{1}H NMR (Scheme 5).

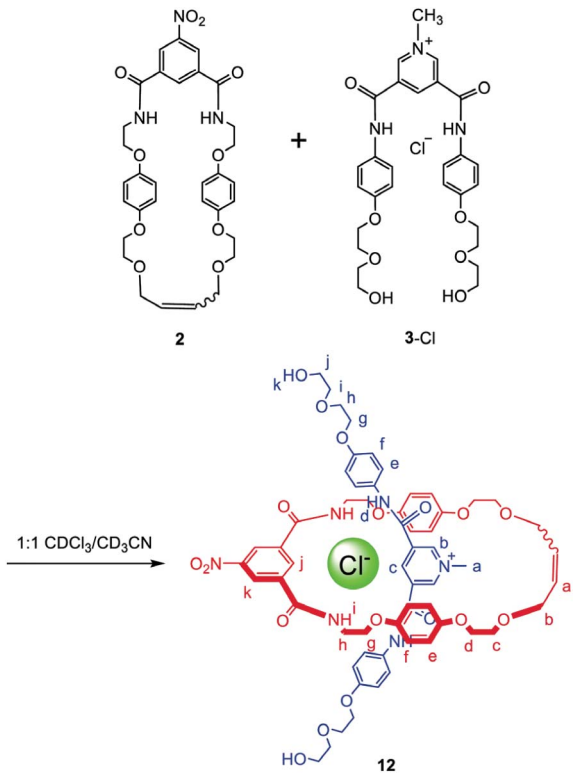

Scheme 5 Pseudorotaxane formation of **2** and **3**-Cl in 1 : 1 $CDCl_3/CD_3CN$.

Upon addition of one equivalent of **3**-Cl to a 1 : 1 $CDCl_3/CD_3CN$ solution of **2**, significant upfield shifts and splitting of the macrocyclic hydroquinone protons H_e ($\Delta\delta = 0.06$ ppm) and H_f ($\Delta\delta = 0.11$ ppm) were observed (Fig. 3), characteristic

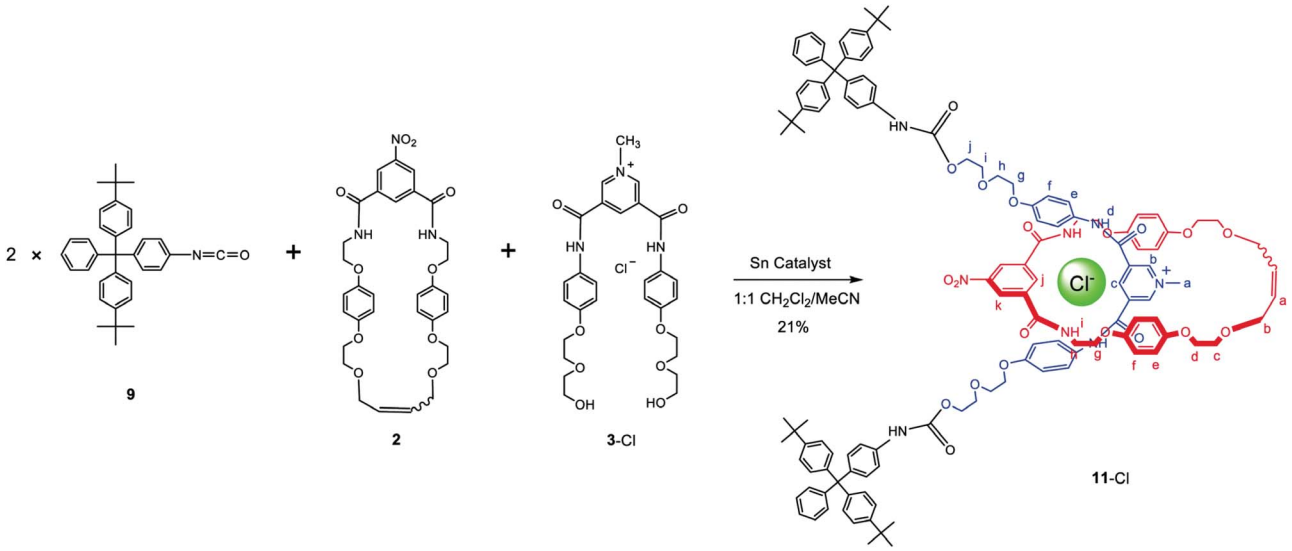

Scheme 6 Rotaxane synthesis of **11**-Cl *via* stoppering strategy.

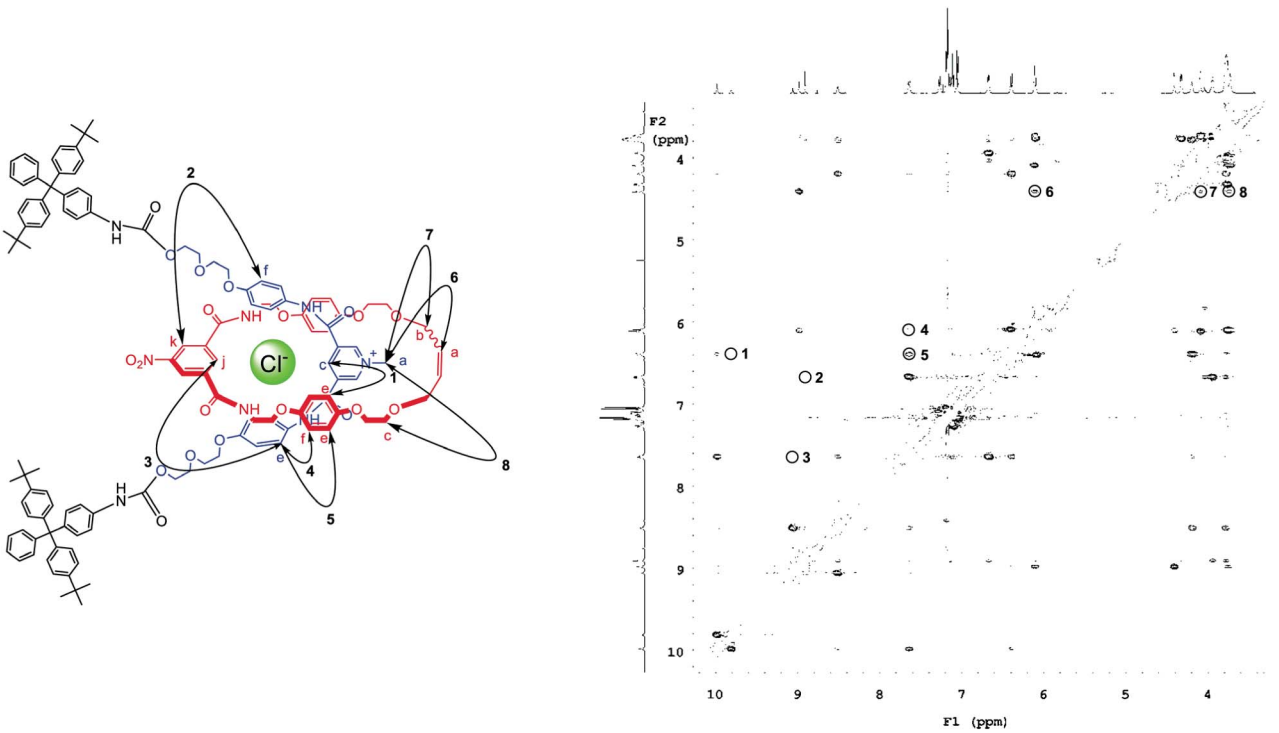

Fig. 2 ROESY spectrum of **11**-Cl in $CDCl_3$ at 298 K, showing the through space correlation between macrocycle and pyridinium axle *via* π–π stacking and hydrogen bonding.

of π–π stacking between the positively charged pyridinium motif and the hydroquinone protons.[9] Chloride anion bound induced downfield shifts were also observed for the macrocycle amide protons H_i ($\Delta\delta = 0.27$ ppm) and aryl protons H_j ($\Delta\delta = 0.18$ ppm) and H_k ($\Delta\delta = 0.01$ ppm) concomitant with upfield shifts of the amide protons H_d ($\Delta\delta = 0.50$ ppm) and aromatic pyridinium proton H_c ($\Delta\delta = 0.35$ ppm) of **3**-Cl, all of which is suggestive of pseudorotaxane formation.

Taking into account the promising results of the pseudorotaxane study, rotaxane synthesis adopting a stoppering strategy was undertaken. An equimolar mixture of **2** and **3**-Cl was stirred in 1 : 1 CH_2Cl_2/MeCN for 1 h to facilitate the assembly of the pseudorotaxane. Two equivalents of isocyanate stopper **9** and a catalytic amount of dibutyl tin dilaurate were then added and the resulting mixture was stirred under N_2 for 72 h. Following workup and column chromatography using 96 : 4 CH_2Cl_2/MeOH as the eluent the target rotaxane **11**-Cl was isolated 21% yield (Scheme 6). The yield of the rotaxane obtained by the stoppering method is significantly lower than that obtained by the clipping method (55%), presumably this is a consequence of the more competitive

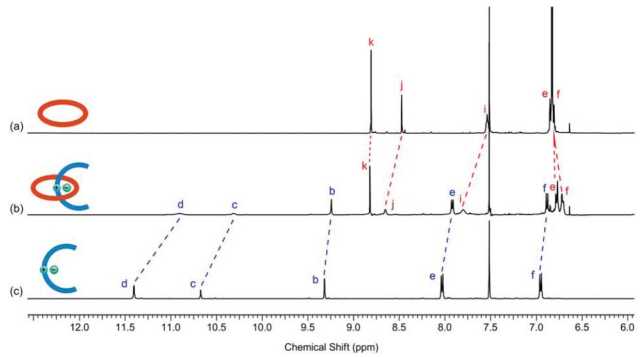

Fig. 3 ^{1}H NMR (500 MHz, 298 K, 1 : 1 $CDCl_3/CD_3CN$) spectra of (a) macrocycle **2**, (b) pseudorotaxane **12**-Cl and (c) pyridinium chloride thread **3**-Cl. For proton labelling see Scheme 5.

CH_2Cl_2/CH_3CN solvent mixture (necessary for the solubility of starting materials) used during the stoppering synthesis.

Anion binding studies

In order to investigate the anion binding properties of the rotaxane, the chloride anion templated was removed by washing a CH_2Cl_2 solution of the chloride salt **11**-Cl with 0.1 M $NH_4PF_{6(aq)}$ to afford hexafluorophosphate salt **11**-PF_6 in quantitative yield.[4] Comparing the ^{1}H NMR spectra of the rotaxane salts in $CDCl_3$, significant upfield shifts of isophthalamide and pyridinium protons were observed in the ^{1}H NMR spectrum of **11**-PF_6 due to the loss of hydrogen bonding interactions with the encapsulated templating chloride anion. Anion exchange was also confirmed by ^{19}F and ^{31}P NMR spectra.

The anion binding properties of rotaxane **11**-PF_6 were initially investigated in the solvent mixture 1 : 1 $CDCl_3/CD_3OD$. Upon addition of one equivalent of chloride, significant downfield shifts of the *para*-pyridinium proton of the axle H_c ($\Delta\delta$ = 0.34 ppm) and *para*-aryl proton of the macrocycle H_j ($\Delta\delta$ = 0.24 ppm) were observed indicating anion complexation. The binding stoichiometry was determined to be 1 : 1 host/anion by Job plot analysis. The titration data analysed by WinEQNMR[10] software reveals that rotaxane **11**-PF_6 complexes Cl^- and Br^- very strongly in this solvent mixture of 1 : 1 $CDCl_3/CD_3OD$ (K_a > 10^4 M^{-1}) (Table 2). In addition **11**-PF_6 exhibits relatively weaker binding with oxoanions such as SO_4^{2-}, HSO_4^-, OAc^- and $H_2PO_4^-$ due to unfavourable size complementarity. In order to quantify the selectivity of rotaxane **11**-PF_6 for these halide anions the titration experiments were repeated in the more competitive aqueous solvent mixture of 45 : 45 : 10 $CD_3OD/CDCl_3/D_2O$. Again, upon addition of one molar equivalent of TBA chloride to the rotaxane, significant downfield shifts of the *para*-pyridinium proton H_c ($\Delta\delta$ = 0.22 ppm) and *para*-aryl proton H_j ($\Delta\delta$ = 0.23 ppm) of **11**-PF_6 were observed (Fig. 4).

Association constants, determined by WinEQNMR analysis of the titration data (Fig. 5), are reported in Table 2. In comparison to macrocycle **2** and axle **4**-BF_4 (Table 1), the anion recognition ability of rotaxane **11**-PF_6 is enhanced dramatically due to the cooperative hydrogen bond donating ability of the rotaxane cavity containing two orthogonal amide clefts. For example, in 45 : 45 : 10 $CD_3OD/CDCl_3/D_2O$, the rotaxane exhibits a significantly stronger binding affinity for Cl^- and Br^- (K_a = 4610 M^{-1} and K_a = 1820 M^{-1} respectively) than macrocycle **2** (no binding) or axle **4**-BF_4 (K_a = 140 M^{-1} and K_a = 120 M^{-1} respectively) which indicates that the rotaxane is clearly a superior anion complexant. In addition, as the templating anion, chloride displays optimal size and geometry complementarity to the topological cavity of the rotaxane, and hence is bound more strongly than other anions. In sharp contrast to **2** and **4**-BF_4, which exhibit high binding affinities for more basic anions (OAc^- > Cl^-), the rotaxane binds dihydrogen phosphate and acetate anions more weakly. The reason is presumably that the rotaxane is unable to present a full complement of hydrogen bond donors for anion complexation to these larger anions, which are sterically prevented from fully penetrating the interlocked binding cavity. Impressively, the rotaxane binds both chloride and bromide more strongly than the sulfate dianion, indicating that the sulfate anion is too large in size to penetrate the interlocked host cavity.

Furthermore, in comparison to [2]rotaxanes reported previously which selectively bind chloride in 1 : 1 $CD_3OD/CDCl_3$ with

Table 1 Association constants (M^{-1}) of macrocycle **2** (determined by *para*-nitro-isophthalamide proton H_j) and axle **4**-BF_4 (determined by *para*-pyridinium proton H_c) with anions in competitive solvents at 298 K (estimated errors less than 10%)

Anion	**2**[a]	**4**-BF_4[a]	**2**[b]	**4**-BF_4[b]
Cl^-	50	475	N.B.	140
Br^-	20	545	N.B.	120
AcO^-	180	905	N.B.	—

[a] In 1 : 1 $CD_3OD/CDCl_3$. [b] In 45 : 45 : 10 $CDCl_3/CD_3OD/D_2O$.

Table 2 Association constants (M^{-1}) of **11**-PF_6 (determined by *para*-pyridinium proton H_c) with anions in competitive solvents at 298 K (estimated errors less than 10%)

Anion	**11**-PF_6[a]	**11**-PF_6[b]
Cl^-	$>10^4$	4610
Br^-	$>10^4$	1820[c]
SO_4^{2-}	8680	1470
F^-	—	850
I^-	—	315
HSO_4^-	765	235
OAc^-	1040[c]	180
$H_2PO_4^-$	355	340

[a] In 1 : 1 $CD_3OD/CDCl_3$. [b] In 45 : 45 : 10 $CDCl_3/CD_3OD/D_2O$. [c] Determined by *ortho*-nitroisophthalamide proton H_c.

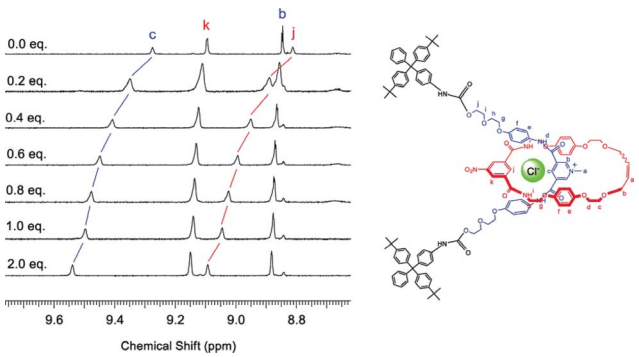

Fig. 4 ^{1}H NMR (500 MHz, 298 K, 45 : 45 : 10 $CDCl_3/CD_3OD/D_2O$) titration spectra of rotaxane **11**-PF_6 with chloride.

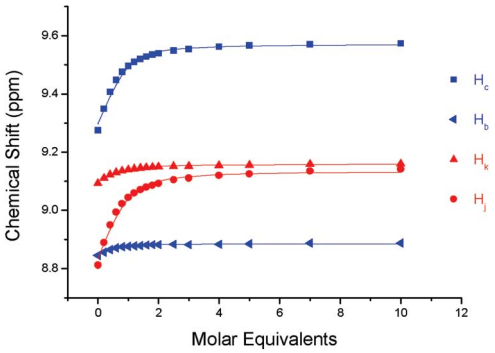

Fig. 5 ^{1}H NMR titration curves of **11**-PF_6 with TBACl in 45 : 45 : 10 $CDCl_3/CD_3OD/D_2O$, monitoring pyridinium protons H_b, H_c and nitro-isophthalamide protons H_j, H_k.

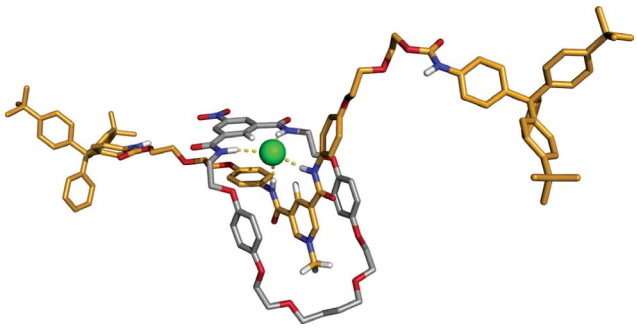

Fig. 6 A representative energy minimised *syn-syn* co-conformation of **11**-Cl complex showing two sets of π–π stacking interactions between the aromatic rings of macrocycle and axle components. The carbon atoms of the motorcycle are in gray and of the axle in orange. The majority of C–H hydrogen atoms have been omitted for clarity and the N–H···Cl hydrogen bonds are drawn as yellow dashed lines.

association constants of up to K_a = 4500 M^{-1},[5] the recognition ability of rotaxane **11**-PF_6 for chloride is significantly enhanced (K_a > 10^4 M^{-1} in 1 : 1 $CD_3OD/CDCl_3$). Even in the aqueous solvent mixture, rotaxane **11**-PF_6 still performs as a superior anion host. This suggests that the novel design of the two sets of π–π stacking interactions between the positively charged electron deficient pyridinium motif and the macrocyclic electron rich hydroquinone groups as well as between the electron-rich aryl groups and the electron-deficient nitro-isophthalamide group of the macrocycle, help preorganise the rotaxane's unique interlocked binding cavity which is of complementary size and shape for selectively binding chloride and bromide in preference to larger oxoanions.

Modelling studies

The anion binding ability of $\mathbf{11}^+$ was also investigated by means of molecular mechanics and molecular dynamics (MD) simulations carried out for Cl^-, Br^-, SO_4^{2-}, OAc^- and $H_2PO_4^-$ anion associations using the AMBER 11 software package.[11] The [2]rotaxane and oxo anions were described with force field parameters taken from GAFF[12] and RESP atomic charges.[13] Remaining computational details are given in the supplementary material.†

The structures of chloride and polyatomic anions assembled with rotaxane **11** were generated in the gas phase *via* a MD quenching approach. Among the 2000 docking co-conformations saved for the **11**-Cl complex, the structures of the most populated cluster revealed a similar binding arrangement as found in other related rotaxane systems.[3d,14] As illustrated in Fig. 6 with a representative structure, the chloride anion establishes concomitantly four N–H···Cl hydrogen bonds with the axle pyridinium motif and macrocyclic nitro-isophthalamide unit, which adopt an orthogonal binding arrangement stabilized by π–π stacking interactions between the pyridinium moiety and the two hydroquinone rings of the macrocycle. In addition, the electron-deficient nitro-isophthalamide cleft is also involved in π–π stacking interactions with one electron-rich oxyaniline group of the thread leading to a three-dimensional rotaxane binding cavity. In conformational analysis no co-conformations involving the simultaneous π–π stacking of the two oxyaniline groups were observed. The molecular mechanics structure of **11**-Cl is entirely consistent with the solution NMR structural findings. Equivalent topological binding scenarios between the polyatomic anions OAc^-, SO_4^{2-} and $H_2PO_4^-$ and **11** were also clustered.

Afterwards, selected low energy structures of rotaxane halide (Cl^- and Br^-) and oxoanion (SO_4^{2-}, OAc^- and $H_2PO_4^-$) complexes were immersed in periodic cubic boxes of a $CHCl_3/CH_3OH/H_2O$ (45 : 45 : 10) explicit solvent mixture and their dynamic structural behaviours were evaluated by MD simulations for 15 ns. The starting structure of **11**-Br complex was obtained from the **11**-Cl counterpart replacing chloride with the bromide anion.

Selected snapshots taken from the MD simulations of rotaxane halide and oxoanion complexes showing the anions surrounded by their 2nd solvent shells (see below) are presented in Fig. 7 and Fig. 8 respectively. In Cl^-, Br^- and OAc^- complexes, the pyridinium and isophthalamide clefts are assembled in an almost orthogonal fashion held by four uninterrupted hydrogen bonds established with the anions. In SO_4^{2-} and $H_2PO_4^-$ associations, the rotaxane orthogonal arrangement is assisted by multiple N–H···O hydrogen bonds based on the intermittent swapping of all the oxygen atom interactions, which contributes to the weakening of the oxoanion-rotaxane binding.

The distances between the pyridinium motif and the hydroquinone rings of the macrocycle ($C_{pyr}\cdots C_{hyd}$) and between the nitro-isophthalamide cleft and the two axle's oxyaniline rings ($C_{iso}\cdots C_{oxy}$) were monitored during the course of MD simulations. The average values with their standard deviations, reported in Table 3, show that the two sets of π–π stacking interactions between the aromatic rings of the macrocycle and axle components found in the gas phase are preserved in solution over the entire time of the MD simulations carried out with the different anions. In addition, the two sets of $C_{iso}\cdots C_{oxy}$ average distances reported, one shorter and other extensively longer (for instance 4.01 and 9.71 Å in the **11**-Cl complex) show that only one axle's electron-rich oxyaniline ring is face-to-face with the electron-deficient nitro-isophthalamide ring of the macrocycle while the other is far away from the rotaxane binding cavity.

The distance from the anion (A^-) to the centre of the binding cavity (C_{N4}), determined by the four nitrogen binding sites from the two amide clefts, was also evaluated and their average values together with the standard deviations are also given in Table 3. The chloride (1.50 Å) is located preferentially inside of the binding pocket whereas the bromide anion (1.65 Å) has a propensity to

Table 3 Average $A\cdots C_{N4}$, $C_{pyr}\cdots C_{hyd}$ and $C_{iso}\cdots C_{oxy}$ distances (Å) with their standard deviations for rotaxane **11**-anion complexes

Anion	$A\cdots C_{N4}$ [a]	$C_{pyr}\cdots C_{hyd}$ [b]	$C_{iso}\cdots C_{oxy}$ [b]
Cl^-	1.50 ± 0.21	3.84 ± 0.37, 3.83 ± 0.34	9.68 ± 0.41, 4.03 ± 0.38
Br^-	1.64 ± 0.21	3.85 ± 0.33, 3.79 ± 0.33	10.09 ± 0.39, 4.02 ± 0.36
OAc^-	1.62 ± 0.17	3.95 ± 0.33, 3.71 ± 0.24	9.65 ± 0.44, 4.07 ± 0.29
SO_4^{2-}	2.55 ± 0.44	4.22 ± 0.34, 3.67 ± 0.20	9.95 ± 0.40, 3.84 ± 0.31
$H_2PO_4^-$	2.52 ± 0.45	3.78 ± 0.30, 3.68 ± 0.23	10.29 ± 0.45, 3.95 ± 0.32

[a] For SO_4^{2-} and $H_2PO_4^-$ anions, A^- represents the S and P respectively, whereas for the OAc^- anion it means the mass centre of the carboxylate group; C_{N4} is the mass centre of the rotaxane binding cavity determined by the four nitrogen donors of the amide clefts. [b] C_{pyr}, C_{hyd}, C_{iso} and C_{oxy} are the mass centres of the pyridinium, nitro-isophthalamide, hydroquinones and oxyaniline aromatic rings respectively. The standard deviations were calculated for $N = 75\,000$.

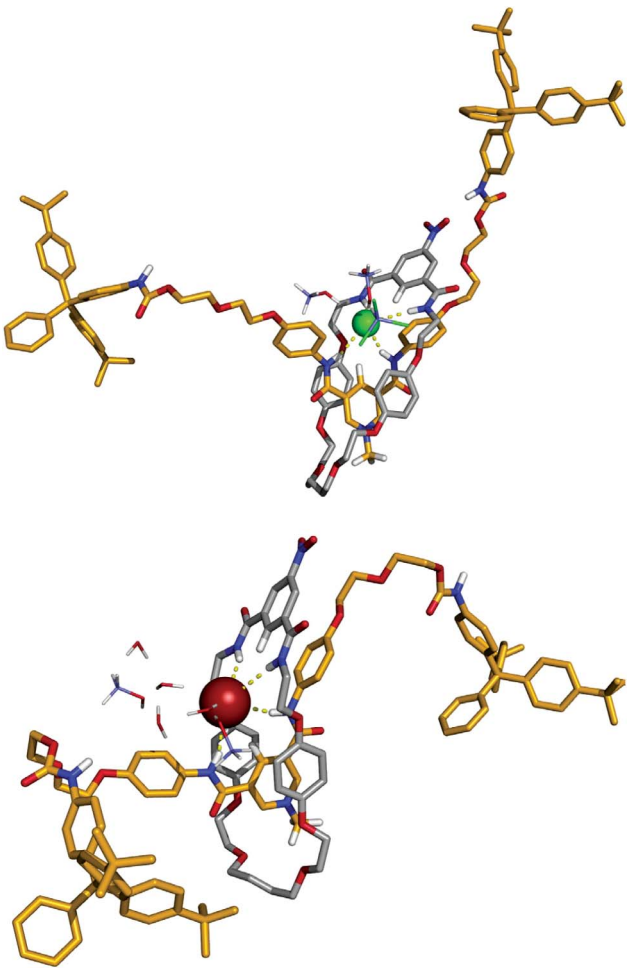

Fig. 7 Selected snapshots of **11**-Cl (top) and **11**-Br (bottom) complexes showing the 2nd anion solvent shell. The methanol and chloroform solvent molecules are drawn as sticks with carbon atoms in slate colour. Remaining details as given in Fig. 6.

remain barely outside of the binding cavity. In contrast, the average distances for sulfate (2.55 Å) and dihydrogen phosphate (2.52 Å) reveal that these polyatomic anions are too large in size to enter into the three-dimensional rotaxane binding cavity. Furthermore, the larger standard deviations of this structural parameter indicate that rotaxane **11** binds these anions weakly. The carboxylate group of the more basic oxoanion OAc^- is on average only 1.62 Å away from the binding cavity. Nevertheless, as with the other two polyatomic anions and in contrast with the monoatomic ones, the

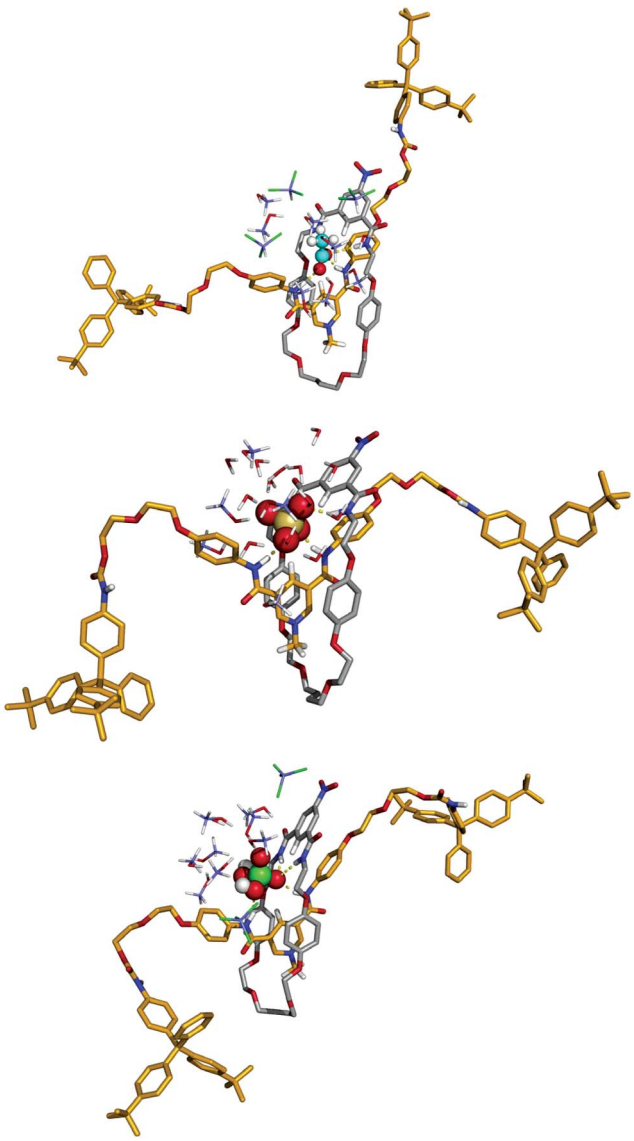

Fig. 8 Illustrative snapshots of **11**-OAc^- (top), **11**-SO_4^{2-} (middle) **11**-$H_2PO_4^-$ (bottom) complexes showing the 2nd anion solvent shell. The acetate is represented in ball and stick mode and the remaining ones as spheres. Remaining details as given in Fig. 6.

acetate methyl group is clearly located outside of the rotaxane binding pocket, as can be seen clearly in Fig. 8. It is noteworthy, that the Cl^- anion having the shorter $A\cdots C_{N4}$ distance is more

Table 4 Average number of solvent molecules (the maximum and minimum number are given within parentheses) enclosing the anions within the 1st and 2nd shells with radii of 3.4 and 5.0 Å respectively[a]

	MeOH		H_2O		$CHCl_3$	
	1st	2nd	1st	2nd	1st	2nd
Cl^-	1.4 (0–4)	3.3 (0–8)	0.9 (0–5)	1.4 (0–8)	0.1 (0–2)	0.4 (0–4)
Br^-	1.6 (0–4)	3.1 (0–8)	0.7 (0–5)	1.2 (0–8)	0.1 (0–2)	0.4 (0–4)
OAc^-	1.1 (0–4)	2.8 (0–9)	0.2 (0–3)	0.5 (0–8)	0.1 (0–2)	1.6 (0–6)
SO_4^{2-}	2.1 (0–6)	4.5 (0–11)	4.9 (1–10)	7.6 (2–16)	0.0 (0–1)	0.1 (0–3)
$H_2PO_4^-$	2.9 (0–8)	5.0 (1–14)	0.5 (0–5)	1.0 (0–9)	1.1 (0–4)	2.6 (0–8)

[a] The distances for polyatomic anions were measured from the centre of mass defined in Table 3.

strongly bonded to the rotaxane system than the remaining anions, which is in agreement with experimental binding data (see Table 2).

Further insights on the binding affinity of **11** for halides and oxoanions can be acquired by counting the number of methanol, water and chloroform molecules of the competitive aqueous solvent mixture around the anions along the MD simulations. The average number of solvent molecules found in the first and the second solvent shells are listed in Table 4.

In rotaxane complexes, apart from sulfate all the anions are preferentially solvated in the first and second solvation shells by methanol molecules. In **11**-SO_4^{2-} association, the anion is mostly surrounded by water molecules in both solvent shells. As would be expected, chloroform solvates poorly the anions and the number of solvent molecules only increases near the solution bulk. This is particularly evident in the second solvent shells of OAc^- and $H_2PO_4^-$ with average number of chloroform molecules of 1.6 and 2.6, respectively. These numbers are understandable taking into account that the methyl acetate group and the phosphate anion are located outside the binding pocket and are therefore exposed to the solvent. However, the cut-off used for the solvent second shell (5.0 Å) is near the solvent bulk approach and the subsequent discussion will be limited to the first methanol and water solvent shells. As shown above, the rotaxane **11** shields the halide anions from the solvent mixture leading to a small average number of methanol molecules of 1.4 for chloride and 1.6 for bromide. In contrast, the inorganic polyatomic anions, located outside of the binding pocket, are exposed to the polar solvents and their solvent shells are composed of a significant number of solvent molecules: 4.9 water molecules for sulfate and 2.9 methanol molecules for dihydrogen phosphate. Naturally, the $A\cdots C_{N4}$ distances and the solvation extension of these two anions follow the same order and consequently the experimental binding preference of **11** for the sulfate anion seems to be dictated by its net charge, in other words, by the strength of the electrostatic interactions between **11** and SO_4^{2-}. The association constants of **11** and SO_4^{2-}, quoted in Table 2, decrease significantly on addition of water to the solvent medium, which is not the case with $H_2PO_4^-$ association. This experimental fact is explained from MD simulations when taking into account the preference of the sulfate anion to be surrounded by a large number of water molecules compared with dihydrogen phosphate, which is preferentially solvated by methanol molecules.

Conclusions

A novel [2]rotaxane, containing nitro-isophthalamide macrocycle and polyether appended pyridinium axle components, has been synthesised *via* both clipping and stoppering synthetic methodologies using an anion templation strategy. The rotaxane is characterised by ^{1}H NMR, ROESY ^{1}H–^{1}H NMR spectroscopy and ESI mass spectrometry. Through space correlation studies reveal that two sets of π–π stacking interactions between the aromatic rings of macrocycle and axle components form a topologically unique three-dimensional binding cavity. This structural feature is corroborated by molecular dynamics simulations carried out in a competitive aqueous solvent medium. After removing the chloride anion template, ^{1}H NMR titration experiments reveal this preorganised interlocked host to be highly selective for binding chloride and bromide in preference to basic oxoanions in competitive aqueous solvent mixtures. The rotaxane host system proved to be a superior anion complexant in comparison to the individual macrocycle and axle components, and other isophthalamide-pyridinium rotaxane systems reported previously. The molecular dynamics structural data show that the superior binding affinity of the rotaxane for chloride and bromide anions in comparison with polyatomic oxoanions can be rationalised by the halide anions penetrating the interlocked binding pocket which protects them from solvent molecules. Since the oxoanions are unable in size to be encapsulated within the binding pocket, the strength of association depends largely on the number of water molecules within the oxoanion solvation shells.

Experimental

Materials and instruments

Dry solvents were obtained by purging with nitrogen and then passing through a MBraun MPSP-800 column. Water was deionised and microfiltered using a Milli-Q® Millipore machine. All tetrabutylammonium (TBA) salts, silver hexafluorophosphate, Grubbs' 2nd generation catalyst were stored in a vacuum desiccator over phosphorus pentoxide prior to use. Triethylamine was distilled from and stored over potassium hydroxide. Thionyl chloride was distilled over triphenyl phosphite. All other solvents and commercial grade reagents were used without further purification unless otherwise noted.

Column chromatography was performed on silica gel (160–200 mesh), and thin-layer chromatography (TLC) was performed on preparative silica gel GF plates with UV254 (1000 microns, Analtech, USA). ^{1}H, ^{13}C, ^{19}F and ^{31}P NMR spectra were recorded on a Varian Mercury VX300 or Varian Unity Plus 500 spectrometer. Mass spectrometry was performed on a Bruker microTOF (ESI) or a Waters Micromass MALDI micro MX (MALDI-TOF) mass spectrometer. Microwave reactions were carried out using a Biotage Initiator 2.0 microwave.

Syntheses

Synthesis of 8. A solution of **7** (0.50 g, 2.5 mmol), 3,5-pyridinedicarboxylic acid (0.21 g, 1.3 mmol), *N*-3-dimethylaminopropyl-*N*′-ethylcarbodiimide hydrochloride (EDC) (0.51 g, 2.7 mmol), 1-hydroxybenzotriazole (HOBt) (0.36 g, 2.7 mmol) and triethylamine (0.5 mL, 3.6 mmol) in 1 : 1 CH_2Cl_2/THF (100 mL) was stirred under N_2 for 24 h. After this time the solvent was concentrated *in vacuo* and the residue was purified by column chromatography using 4 : 1 CH_2Cl_2/MeOH as the eluent to give

the pure product as a pale white solid (0.31 g, 47%); ^{1}H NMR (300 MHz, DMSO-d_6, 298 K): δ 10.49 (2H, s, -N*H*-), 9.23 (2H, d, ^4J = 1.8 Hz, Ar*H*), 8.79 (1H, t, $^4J_1$ = 2.1 Hz, $^4J_2$ = 3.7 Hz Ar*H*), 7.69 (4H, d, ^3J = 9.1 Hz, Ar*H*), 6.97 (4H, d, ^3J = 9.1 Hz, Ar*H*), 4.65 (4H, t, -O*H*-), 4.10–4.07 (4H, m, -CH_2-), 3.76–3.73 (4H, m, -CH_2-), 3.52–3.49 (8H, m, -CH_2-); ^{13}C NMR (75 MHz, DMSO-d_6, 298 K): δ 163.4, 155.5, 151.2, 134.9, 132.3, 130.7, 122.4, 114.9, 72.9, 69.4, 67.7, 60.7; ESI-MS (*m*/*z*): [M + Na]$^+$ 548.2004, $C_{27}H_{31}N_3O_8Na$ (calc. 548.2003).

Synthesis of 3-I. Compound **8** (0.30 g, 0.57 mmol) was dissolved in excess iodomethane (5 mL) and acetone (20 mL) and was refluxed under N_2 for 48 h. After this time, diethyl ether (50 mL) was added and the filtration was isolated to give the pure product as a yellow solid (0.35 g, 92%); ^{1}H NMR (300 MHz, DMSO-d_6, 298 K): δ 11.09 (2H, s, -N*H*-), 9.68 (2H, s, Ar*H*), 9.23 (1H, s, Ar*H*), 7.77 (4H, d, ^3J = 9.1 Hz, Ar*H*), 7.02 (4H, d, ^3J = 9.1 Hz, Ar*H*), 4.65 (2H, t, -O*H*-), 4.49 (3H, s, -CH_3-), 4.12–4.09 (4H, m, -CH_2-), 3.76–3.73 (4H, m, -CH_2-), 3.53–3.48 (8H, m, -CH_2-); ^{13}C NMR (125 MHz, CD_3OD, 298 K): δ 160.7, 157.7, 148.3, 142.7, 133.5, 132.1, 123.7, 115.8, 73.8, 70.7, 68.9, 62.2, 49.9; ESI-MS (*m*/*z*): [M - I]$^+$ 540.2354, $C_{28}H_{34}N_3O_8$ (calc. 540.2340).

Synthesis of 3-Cl. A solution of **3**-I (0.35 g, 0.52 mmol) in 2 : 1 MeOH/MeCN (20 mL) was run through a chloride activated amberlite column using the same solvent as the eluent to give the pure product as a bright yellow solid (0.30 g, 99%); ^{1}H NMR (300 MHz, DMSO-d_6, 298 K): δ 11.25 (2H, s, -N*H*-), 9.84 (1H, s, Ar*H*), 9.70 (2H, s, Ar*H*), 7.82 (4H, d, ^3J = 9.1 Hz, Ar*H*), 7.01 (4H, d, ^3J = 9.1 Hz, Ar*H*), 4.66 (2H, t, -O*H*), 4.49 (3H, s, -CH_3-), 4.12–4.09 (4H, m, -CH_2-), 3.76–3.73 (4H, m, -CH_2-), 3.53–3.48 (8H, m, -CH_2-); ^{13}C NMR (75 MHz, CD_3OD, 298 K): δ 160.5, 157.6, 148.3, 142.4, 135.6, 132.2, 123.5, 115.7, 73.8, 70.7, 68.9, 62.2, 49.7; ESI-MS (*m*/*z*): [M - Cl]$^+$ 540.2343, $C_{28}H_{34}N_3O_8$ (calc. 540.2340).

Synthesis of 10. A solution of isocyanate stopper **9** (0.990 g, 2.09 mmol), pyridyl thread **8** (0.501 g, 0.950 mmol) and dibutyltin dilaurate (Sn catalyst) (0.198 g, 0.310 mmol) in 1 : 1 CH_2Cl_2/MeCN (150 mL) was stirred under N_2 for 72 h. The solvent was then removed *in vacuo* and the residue was purified by column chromatography using ethyl acetate as the eluent to give the pure product as a yellow solid (1.02 g, 73%); ^{1}H NMR (500 MHz, $CDCl_3$, 298 K): δ 9.12 (4H, s, -N*H*-), 8.44 (1H, s, Ar*H*), 7.56 (2H, s, Ar*H*), 7.37 (4H, d, ^3J = 8.3 Hz, Ar*H*), 7.27–7.08 (26H, m, Ar*H*), 6.62 (4H, d, ^3J = 8.8 Hz, Ar*H*), 4.28 (4H, m, -CH_2-), 3.91 (4H, m, -CH_2-), 3.74 (8H, m, -CH_2-), 1.25 (36H, s, ^{t}*Bu*); ^{13}C NMR (125 MHz, $CDCl_3$, 298 K): δ 163.3, 155.6, 153.5, 150.3, 148.4, 147.1, 143.7, 142.2, 135.6, 134.4, 131.7, 131.7, 131.0, 130.6, 130.1, 127.3, 125.7, 124.2, 122.7, 117.5, 114.5, 69.6, 69.4, 67.3, 63.7, 63.6, 34.2, 31.3; ESI-MS (*m*/*z*): [M + Na]$^+$ 1494.7449, $C_{95}H_{101}N_5O_{10}Na$ (calc. 1494.7441).

Synthesis of 4-BF_4. Pyridine stoppered thread **10** (0.265 g, 0.180 mmol) and trimethyloxonium tetrafluoroborate (0.040 g, 0.270 mmol) were dissolved in dry dichloromethane and stirred under N_2 for 48 h. After this time, methanol (10 mL) was added to the reaction mixture and the solvent was removed *in vacuo*. The residue was purified by column chromatography using 10 : 1 CH_2Cl_2/MeOH as the eluent to give the pure product as a yellow solid (0.260 g, 92%); ^{1}H NMR (300 MHz, $CDCl_3$, 298 K): δ 10.53 (2H, s, -N*H*-), 9.94 (1H, s, Ar*H*), 9.14 (2H, s, Ar*H*), 7.70 (4H, d, ^3J = 8.5 Hz, Ar*H*), 7.41 (2H, s, -N*H*-), 7.27–7.05 (26H, m, Ar*H*), 6.67 (4H, d, ^3J = 8.8 Hz, Ar*H*), 4.36 (3H, s, -NCH_3), 4.31 (4H, m, -CH_2-), 3.90 (4H, m, -CH_2-), 3.73 (8H, m, -CH_2-), 1.26 (36H, s, ^{t}*Bu*); ^{13}C NMR (125 MHz, $CDCl_3$, 298 K): δ 158.2, 155.9, 153.5, 148.4, 147.2, 146.4, 143.7, 142.3, 135.6, 134.0, 131.7, 131.1, 130.6, 127.3, 125.7, 124.2, 122.3, 117.6, 114.5, 110.0, 69.8, 69.6, 64.7, 64.1, 63.6, 49.2, 43.3, 31.4; ^{19}F NMR (282 MHz, $CDCl_3$, 298 K): δ –148.42; ESI-MS (*m*/*z*): [M – BF_4]$^+$ 1486.7782, $C_{96}H_{104}N_5O_{10}$ (calc. 1487.7778).

Synthesis of 4-Cl. A solution of **4**-BF_4 (0.260 g, 0.165 mmol) in chloroform (50 mL) was washed with saturated $NH_4Cl_{(aq)}$ (5 × 50 mL). The organic phase was dried over magnesium sulfate, filtered and the solvent removed *in vacuo* to give the pure product as a yellow solid (0.250 g, 99%); ^{1}H NMR (500 MHz, $CDCl_3$, 298 K): δ 11.82 (4H, s, -N*H*-), 10.44 (1H, s, Ar*H*), 9.15 (2H, s, Ar*H*), 7.85 (4H, d, ^3J = 8.5 Hz, Ar*H*), 7.24–7.07 (26H, m, Ar*H*), 6.85 (4H, d, ^3J = 9.1 Hz, Ar*H*), 4.37 (3H, s, -CH_3-), 4.34–4.32 (4H, m, -CH_2-), 4.07–4.05 (4H, m, -CH_2-), 3.83–3.81 (4H, m, -CH_2-), 3.79–3.77 (4H, m, -CH_2-), 1.24 (36H, s, ^{t}*Bu*); ^{13}C NMR (125 MHz, $CDCl_3$, 298 K): δ 207.0, 158.6, 155.8, 153.5, 148.4, 147.2, 146.1, 143.7, 142.3, 135.5, 135.1, 131.7, 131.4, 131.1, 130.6, 127.3, 125.7, 124.2, 122.5, 117.5, 114.5, 69.6, 67.5, 64.1, 63.6, 48.9, 34.3, 31.3; ESI-MS (*m*/*z*): [M – Cl]$^+$ 1487.7320, $C_{96}H_{105}N_5O_{10}$ (calc. 1487.7856).

Synthesis of 11-Cl by clipping method. **2** (0.0670 g, 0.103 mmol) and **4**-Cl (0.156 g, 0.103 mmol) were dissolved in dry dichloromethane (20 mL) and stirred under N_2 for 30 min. Grubbs' catalyst 2nd generation (5 mg) was then added and the mixture was stirred for 48 h. The solvent was removed *in vacuo* and the residue was purified by column chromatography using 96 : 4 CH_2Cl_2/MeOH as the eluent to give the pure product as a yellow solid (0.121 g, 55%).

Synthesis of 11-Cl by stoppering method. A solution of **2** (0.0617 g, 0.0993 mmol) and **3**-Cl (0.0572 g, 0.0993 mmol) in 1 : 1 CH_2Cl_2/MeCN (20 mL) was stirred under N_2 for one hour. Isocyanate stopper **9** (0.0943 g, 0.199 mmol) and dibutyltin dilaurate (Sn catalyst) (0.0630 g, 0.0995 mmol) were then added and the mixture was stirred under N_2 for 72 h. After this time the solvent was removed *in vacuo* and the residue was purified by column chromatography column using 25 : 1 CH_2Cl_2/MeOH as the eluent to give the pure product as a yellow solid (44.7 mg, 21%); ^{1}H NMR (500 MHz, $CDCl_3$, 298 K): δ 10.08 (2H, s, -N*H*-), 9.93 (1H, s, Ar*H*), 9.12 (1H, s, NO_2-Ar*H*), 8.99 (2H, s, NO_2-Ar*H*), 8.97 (2H, s, Ar*H*), 8.56 (2H, s, -N*H*-), 7.71 (4H, d, ^3J = 8.8 Hz, Ar*H*), 7.32–7.09 (34H, m, Ar*H*), 6.75 (4H, d, ^3J = 9.3 Hz, Ar*H*), 6.45 (4H, d, ^3J = 8.8 Hz, Ar*H*), 6.18–6.17 (2H, m, C*H*=C*H*), 6.15 (4H, d, ^3J = 8.8 Hz, Ar*H*), 4.49 (3H, s, -CH_3), 4.37–4.35 (4H, m, -CH_2-), 4.25–4.23 (4H, m, -CH_2-), 4.14–4.13 (4H, m, -CH_2-), 4.00–3.99 (4H, m, -CH_2-), 3.83–3.77 (20H, m, -CH_2-), 1.26 (36H, s, -CH_3); ^{13}C NMR (125 MHz, $CDCl_3$, 298 K): δ 164.3, 158.3, 156.7, 153.5, 153.3, 152.0, 148.5, 148.3, 147.1, 145.4, 143.7, 142.2, 136.9, 135.6, 135.1, 133.5, 131.7, 131.1, 130.6, 129.7, 129.0, 127.2, 125.9, 125.6, 124.1, 117.5, 115.5, 115.2, 114.8, 114.5, 114.4, 70.8, 69.7, 69.5, 69.4, 68.1, 67.6, 65.0, 64.2, 63.6, 49.2, 41.4, 34.2, 31.3; ESI-MS (*m*/*z*): [M – Cl]$^+$ 2109.0201, $C_{128}H_{140}N_8O_{20}$ (calc. 2109.0133).

Synthesis of 11-PF_6. A solution of **11**-Cl (0.085 g, 0.040 mmol) in chloroform (5 mL) was washed with 0.1 M $NH_4PF_{6(aq)}$

(10 × 2 mL) and water (2 × 2 mL). The organic layer was dried over magnesium sulfate, filtered and the solvent removed *in vacuo* to give the pure product as a yellow solid (0.086, 96%); ^{1}H NMR (500 MHz, 1 : 1 $CDCl_3/CD_3OD$, 298 K): δ 9.28 (1H, s, NO_2-Ar*H*), 9.10 (2H, s, Ar*H*), 8.83–8.81 (3H, s, Ar*H* & NO_2-Ar*H*), 7.57 (4H, m, Ar*H*), 7.29–7.07 (34H, m, Ar*H*), 6.81 (4H, m, Ar*H*), 6.49 (4H, d, ^3J = 8.8 Hz, Ar*H*), 6.36 (4H, d, ^3J = 9.2 Hz, Ar*H*), 6.08–6.07 (2H, m, C*H*═C*H*), 4.48 (3H, s, N-CH_3), 4.31–4.30 (4H, m, -CH_2-), 4.13–4.11 (4H, m, -CH_2-), 4.08–4.06 (4H, m, -CH_2-), 4.04–4.02 (4H, m, -CH_2-), 3.90–3.99 (4H, m, -CH_2-), 3.84–3.79 (12H, m, -CH_2-), 3.74–3.72 (4H, m, -CH_2-), 1.27 (36H, s, -CH_3); ^{13}C NMR (125 MHz, $CDCl_3$, 298 K): δ 164.8, 158.6, 156.6, 153.5, 152.4, 151.9, 148.5, 148.4, 147.1, 144.9, 143.7, 142.3, 135.5, 135.3, 133.9, 133.5, 131.7, 131.1, 130.6, 130.5, 129.8, 127.2, 125.9, 125.7, 124.2, 117.5, 115.2, 115.2, 115.1, 114.8, 114.5, 70.8, 69.7, 69.5, 69.2, 67.5, 66.0, 64.1, 63.6, 62.7, 49.3, 40.3, 34.3, 31.3; ^{19}F NMR (282 MHz, $CDCl_3$, 298 K): δ −70.22 (6F, *d*, ^1J = 713.4 Hz, PF_6^-); ^{31}P NMR (121 MHz, $CDCl_3$, 298 K): δ 156.27 (*quint*, ^1J = 714.5 Hz, *P*F_6^-); ESI-MS (*m*/*z*): $[M - PF_6]^+$ 2108.9616, $C_{128}H_{140}N_8O_{20}$ (calc. 2109.0133).

^{1}H NMR titration protocol

All NMR titration experiments were conducted on an Oxford Instruments Varian Unity Plus 500 MHz spectrometer, at 298 K. Initial sample volumes were 600 μL. The starting concentration of the host was 2 mM for all titrations. All anions were added as their TBA salts (0.06 M in 1.0 mL). 17 aliquots of the TBAX solutions (corresponding to 0, 0.2, 0.4, 0.6, 0.8, 1.0, 1.2, 1.4, 1.6, 1.8, 2.0, 2.5, 3.0, 4.0, 5.0, 7.0, 10.0 equivalents of added guest) were added until a total of 10 equivalents of the anion had been added. Spectra were recorded after each addition, and the sample shaken thoroughly before measurement.

Stability constants were obtained by analysis of the resulting titration data using the WinEQNMR[10] computer program. Estimates for each binding constant, the limiting chemical shifts and the complex stoichiometry were also added to the input file. The various parameters were refined by non-linear least-squares analysis to achieve the best fit between observed and calculated chemical shifts. The parameters were varied until the values for the stability constants converged. Comparison of the calculated binding isotherm with that obtained experimentally demonstrated that the model used was appropriate.

Acknowledgements

We thank WEILUN, CGA and GBCC for scholarships (Y.L.) and the EPSRC for a post-doctoral fellowship (K.M.M.). We also thank Dr N. H. Rees for valuable NMR advice. Vítor Félix (V.F.) acknowledges the FCT for financial support under project PTDC/QUI/68582/2006 with co-participation European Community funds from the FEDER, QREN and COMPET.

Notes and references

1 (*a*) F. Li, J. K. Clegg, L. F. Lindoy, R. B. Macquart and G. V. Meehan, *Nat. Commun.*, 2011, **2**, 205; (*b*) J. F. Stoddart, *Chem. Soc. Rev.*, 2009, **38**, 1802–1820; (*c*) K. M. Mullen and P. D. Beer, *Chem. Soc. Rev.*, 2009, **38**, 1701–1713; (*d*) J. D. Crowley, S. M. Goldup, A. L. Lee, D. A. Leigh and R. T. McBurney, *Chem. Soc. Rev.*, 2009, **38**, 1530–1541; (*e*) D. B. Amabilino and L. Perez-Garcia, *Chem. Soc. Rev.*, 2009, **38**, 1562–1571; (*f*) B. Champin, P. Mobian and J. P. Sauvage, *Chem. Soc. Rev.*, 2007, **36**, 358–366; (*g*) E. R. Kay, D. A. Leigh and F. Zerbetto, *Angew. Chem., Int. Ed.*, 2007, **46**, 72–191; (*h*) C. Dietrich-Buchecker and J.-P. Sauvage, *Molecular Catenanes, Rotaxanes and Knots. A Journey Through the World of Molecular Topology*, vol. 10, Wiley-VCH, Weinheim, Germany, 1999.

2 (*a*) X. Ma and H. Tian, *Chem. Soc. Rev.*, 2010, **39**, 70–80; (*b*) L. Fang, M. A. Olson, D. Benitez, E. Tkatchouk, W. A. Goddard and J. F. Stoddart, *Chem. Soc. Rev.*, 2010, **39**, 17–29; (*c*) M. D. Lankshear and P. D. Beer, *Acc. Chem. Res.*, 2007, **40**, 657–668; (*d*) A. Marquis, V. Smith, J. Harrowfield, J. M. Lehn, H. Herschbach, R. Sanvito, E. Leize-Wagner and A. Van Dorsselaer, *Chem.–Eur. J.*, 2006, **12**, 5632–5641; (*e*) V. Amendola, M. Boiocchi, B. Colasson, L. Fabbrizzi, E. Monzani, M. J. Douton-Rodriguez and C. Spadini, *Inorg. Chem.*, 2008, **47**, 4808–4816; (*f*) C. D. Pentecost, K. S. Chichak, A. J. Peters, G. W. V. Cave, S. J. Cantrill and J. F. Stoddart, *Angew. Chem., Int. Ed.*, 2007, **46**, 218–222; (*g*) K. S. Chichak, S. J. Cantrill, A. R. Pease, S. H. Chiu, G. W. V. Cave, J. L. Atwood and J. F. Stoddart, *Science*, 2004, **304**, 1308–1312.

3 (*a*) A. J. McConnell and P. D. Beer, *Chem.–Eur. J.*, 2011, **17**, 2724–2733; (*b*) L. M. Hancock, L. C. Gilday, N. L. Kilah, C. J. Serpell and P. D. Beer, *Chem. Commun.*, 2011, **47**, 1725–1727; (*c*) A. J. McConnell, C. J. Serpell, A. L. Thompson, D. R. Allan and P. D. Beer, *Chem.–Eur. J.*, 2010, **16**, 1256–1264; (*d*) D. E. Phipps and P. D. Beer, *Tetrahedron Lett.*, 2009, **50**, 3454–3457; (*e*) L. M. Hancock and P. D. Beer, *Chem.–Eur. J.*, 2009, **15**, 42–44; (*f*) A. Brown, K. M. Mullen, J. Ryu, M. J. Chmielewski, S. M. Santos, V. Felix, A. L. Thompson, J. E. Warren, S. I. Pascu and P. D. Beer, *J. Am. Chem. Soc.*, 2009, **131**, 4937–4952; (*g*) K. Y. Ng, V. Felix, S. M. Santos, N. H. Rees and P. D. Beer, *Chem. Commun.*, 2008, 1281–1283; (*h*) B. Q. Huang, S. M. Santos, V. Felix and P. D. Beer, *Chem. Commun.*, 2008, 4610–4612; (*i*) M. J. Chmielewski, L. Y. Zhao, A. Brown, D. Curiel, M. R. Sambrook, A. L. Thompson, S. M. Santos, V. Felix, J. J. Davis and P. D. Beer, *Chem. Commun.*, 2008, 3154–3156; (*j*) P. D. Beer, M. R. Sambrook and D. Curiel, *Chem. Commun.*, 2006, 2105–2117; (*k*) M. J. Chmielewski, J. J. Davis and P. D. Beer, *Org. Biomol. Chem.*, 2009, **7**, 415–424.

4 K. M. Mullen, J. Mercurio, C. J. Serpell and P. D. Beer, *Angew. Chem., Int. Ed.*, 2009, **48**, 4781–4784.

5 M. R. Sambrook, P. D. Beer, M. D. Lankshear, R. F. Ludlow and J. A. Wisner, *Org. Biomol. Chem.*, 2006, **4**, 1529–1538.

6 (*a*) K. Y. Ng, A. R. Cowley and P. D. Beer, *Chem. Commun.*, 2006, 3676–3678; (*b*) M. R. Sambrook, P. D. Beer, J. A. Wisner, R. L. Paul, A. R. Cowley, F. Szemes and M. G. B. Drew, *J. Am. Chem. Soc.*, 2005, **127**, 2292–2302; (*c*) M. R. Sambrook, P. D. Beer, J. A. Wisner, R. L. Paul and A. R. Cowley, *J. Am. Chem. Soc.*, 2004, **126**, 15364–15365; (*d*) J. A. Wisner, P. D. Beer, M. G. B. Drew and M. R. Sambrook, *J. Am. Chem. Soc.*, 2002, **124**, 12469–12476; (*e*) J. A. Wisner, P. D. Beer, N. G. Berry and B. Tomapatanaget, *Proc. Natl. Acad. Sci. U. S. A.*, 2002, **99**, 4983–4986; (*f*) J. A. Wisner, P. D. Beer and M. G. B. Drew, *Angew. Chem., Int. Ed.*, 2001, **40**, 3606–3609.

7 H. W. Gibson, S. H. Lee, P. T. Engen, P. Lecavalier, J. Sze, Y. X. Shen and M. Bheda, *J. Org. Chem.*, 1993, **58**, 3748–3756.

8 (*a*) C. Hamann, J. M. Kern and J. P. Sauvage, *Inorg. Chem.*, 2003, **42**, 1877–1883; (*b*) M. Scholl, S. Ding, C. W. Lee and R. H. Grubbs, *Org. Lett.*, 1999, **1**, 953–956; (*c*) C. Dietrich-Buchecker, G. Rapenne, J. P. Sauvage, in *XXXIII International Conference on Coordination Chemistry*, Elsevier Science Sa, Florence, Italy, 1998, 167–176; (*d*) R. H. Grubbs, S. J. Miller and G. C. Fu, *Acc. Chem. Res.*, 1995, **28**, 446–452.

9 (*a*) S. J. Loeb and J. A. Wisner, *Chem. Commun.*, 2000, 845–846; (*b*) B. L. Allwood, H. Shahriarizavareh, J. F. Stoddart and D. J. Williams, *J. Chem. Soc., Chem. Commun.*, 1987, 1058–1061; (*c*) J. E. Kickham, S. J. Loeb and S. L. Murphy, *Chem.–Eur. J.*, 1997, **3**, 1203–1213.

10 M. J. Hynes, *J. Chem. Soc., Dalton Trans.*, 1993, 311–312.

11 D. A. Case *et al.*, AMBER 11, University of California, San Francisco, 2010.

12 J. Wang, R. M. Wolf, J. W. Caldwell, P. A. Kollmann and D. A. Case, *J. Comput. Chem.*, 2004, **25**, 1157–1174 .

13 T. Fox and P. A. Kollman, *J. Phys. Chem. B*, 1998, **102**(41), 8070–8079.

14 L. M. Hancock, L. C. Gilday, S. Carvalho, P. J. Costa, V. Félix, C. J. Serpell, N. L. Kilah and P. D. Beer, *Chem.–Eur. J.*, 2010, **16**, 13082–13094.

